

Meiotic Synapsis Proceeds from a Limited Number of Subtelomeric Sites in the Human Male

Petrice W. Brown,^{1,2,*} LuAnn Judis,^{1,2} E. Ricky Chan,^{1,2} Stuart Schwartz,^{1,2} Allen Seftel,³ Anthony Thomas,⁴ and Terry J. Hassold^{1,2,*}

¹Center for Human Genetics and Departments of ²Genetics and ³Urology, Case Western Reserve University School of Medicine and University Hospitals of Cleveland, and ⁴Glickman Urological Institute, Cleveland Clinic Foundation, Cleveland

The formation of the synaptonemal complex (SC) is a crucial early step in the meiotic process, but relatively little is known about the establishment of the human SC. Accordingly, we recently initiated a study of synapsis in the human male, combining immunofluorescence and fluorescence in situ hybridization methodologies to analyze prophase spermatocytes from a series of control individuals. Our results indicate that synapsis is a tightly regulated process, with relatively little variation among individuals. On nonacrocentric chromosomes, there are two synaptic initiation sites, one on the distal short arm and one on the distal long arm, whereas acrocentric chromosomes exhibit a single site on the distal long arm. For both types of chromosomes, synapsis then proceeds toward the centromere, with little evidence that specific p- or q-arm sequences affect the process. However, the centromere appears to have an inhibitory effect on synapsis—that is, when one arm of a nonacrocentric chromosome is “zippered up” before the other, the centromere acts as a barrier to further movement from that arm.

Introduction

Meiosis is the specialized cellular division that, after one round of DNA replication and two divisions, transforms diploid cells into haploid gametes. The first stage of meiosis I, prophase, involves a complex series of chromosomal interactions required for homologous chromosome pairing, synapsis, and recombination (e.g., see Zickler and Kleckner 1999). Over the past 10–15 years, studies of model organisms have made it clear that mutations affecting any of these processes can lead to meiotic arrest or the generation of genetically abnormal gametes (Sym and Roeder 1994; Yuan et al. 2000, 2002; Page and Hawley 2001; Hunt and Hassold 2002). However, the impact of these errors on human meiosis is much less certain. To be sure, altered levels or positioning of recombination events has been linked to human aneuploidy (Hassold and Hunt 2001). However, the contribution of errors in either pairing or synapsis to meiotic arrest and/or chromosome malsegregation has yet to be fully documented.

As part of ongoing studies of human meiosis, our laboratory has been interested in characterizing the syn-

aptic process, the physical association of homologous chromosomes that is mediated by a tripartite, proteinaceous structure: the synaptonemal complex (SC). The SC is a highly conserved, meiosis-specific structure found in most eukaryotic organisms, including budding yeast, flies, worms, and mammals. The mature SC is composed of two axial elements, which are bound to the DNA of each homolog, and the central transverse filament, which connects the two axial elements (which are then referred to as “lateral elements”) (Holm and Rasmussen 1977; Schmekel and Daneholt 1998; Yuan et al. 2000).

Studies of model organisms indicate a link between disruption of synapsis and downstream meiotic abnormalities, including decreased levels of recombination and/or increases in nondisjunction. For example, in *Drosophila melanogaster* mutants that lack a functional copy of *c(3)G*, a key component of the transverse filament, the SC fails to form and crossing-over is eliminated (Page and Hawley 2001; Anderson et al. 2005). In mammals, mice homozygous for a null mutation in the gene encoding the axial-element protein SCP3 (MIM 604759) are either infertile because of meiotic arrest at zygotene (males) or subfertile with an increased incidence of aneuploid gametes (females); neither the males nor the females are capable of forming complete SCs (Yuan et al. 2000, 2002). Thus, in both organisms, meiotic errors in synapsis have similar downstream consequences: either meiotic arrest and infertility or aneuploid products.

Presumably, synaptic defects contribute to infertility and aneuploidy in humans as well, but practical prob-

Received May 24, 2005; accepted for publication July 18, 2005; electronically published August 16, 2005.

Address for correspondence and reprints: Dr. Terry Hassold, School of Molecular Biosciences, 542 Fulmer Hall, Washington State University, Pullman, WA 99164. E-mail: terryhassold@wsu.edu

* Present affiliation: School of Molecular Biosciences, Washington State University, Pullman.

© 2005 by The American Society of Human Genetics. All rights reserved. 0002-9297/2005/7704-0005\$15.00

Table 1**Summary of Patient Information**

PATIENT	AGE (years)	REASON FOR ASCERTAINMENT	CHROMOSOME CONSTITUTION	Yq MICRODELETION	NO. OF CELLS SCORED AT	
					Leptotene	Zygotene
Sp370	32	Postvasectomy	46,XY	No deletion	4	11
Sp389	?	?	?	?	...	8
Sp393	31	CBAVD	46,XY	No deletion	...	36
Sp401	43	Postvasectomy	46,XY	No deletion	1	68
Sp403	31	Postvasectomy	46,XY	No deletion	7	41
Sp407	26	CBAVD	46,XY	No deletion	4	67
Sp1006	39	Epididymal obstruction ^a	?	?	<u>14</u>	<u>55</u>
Total					30	286

^a Associated with multiple surgeries.

lems have impeded our ability to investigate this possibility. In part, this reflects the difficulties associated with acquisition of the appropriate meiotic material—that is, fetal ovaries for females and testicular material for males. However, there have also been methodological limitations, including the inability to simultaneously visualize chromosomes and chromosome-associated proteins in meiotic prophase. Thus, although there have been several light and electron microscopic analyses of human male and female meiosis over the past 25 years (Holm and Rasmussen 1977; Wallace and Hultén 1983; Speed 1984; Speed and Chandley 1990; Barlow and Hultén 1998), the basic meiosis I program of chromosome-chromosome and chromosome-protein interactions has yet to be detailed.

Fortunately, recent advances in molecular cytogenetic and immunofluorescence methodologies now make it possible to overcome this limitation. Specifically, by use of appropriate antibodies, the different substages of prophase can be distinguished and analyzed. Further, by coupling this approach with FISH-based analyses of individual chromosomes or chromosome regions (e.g., telomeres or centromeres), it becomes possible to characterize the temporal interactions between homologous chromosomes and chromosome-associated proteins.

In the present study, we have used this strategy to address three basic issues regarding synapsis in the human male—specifically, the extent of variation in synaptic patterns within and among individuals, the location and number of synaptic initiation sites per chromosome, and the kinetics of synapsis. Our analyses of >300 leptotene- or zygotene-stage cells from seven control males indicate that synapsis is a highly regulated event that shows relatively little variation within or among individuals. Indeed, in all individuals and for all chromosomes, synapsis appears to initiate in subtelomeric regions and to proceed proximally toward the centromere. However, against this background, there are clear chromosome-specific differences, with nonacrocentric chromosomes handling synapsis differently than

the acrocentric ones do. Further, chromosome regions influence the extent and kinetics of synapsis, since centromeric sequences appear to act as a barrier to synaptic progression across chromosome arms.

Material and Methods

Sample Population

Testicular samples were obtained from six individuals attending the University Hospitals of Cleveland's Department of Urology or the Glickman Urological Institute of the Cleveland Clinic Foundation for treatment of infertility (table 1). The ages of the individuals ranged from 26 to 43 years. All had been diagnosed with obstructive azoospermia: three because of a previous vasectomy, two because of a congenital bilateral absence of the vas deferens (CBAVD [MIM 277180]) in association with mutations in the *CFTR* gene, and one because of extensive scarring attributable to multiple surgeries. Blood samples were available from five of the six individuals. Karyotypic analysis indicated a normal male (46,XY) chromosomal constitution in all instances, and routine histological analysis indicated normal levels of spermatogenesis in all individuals. STS-based assays for Yq microdeletions failed to detect any abnormalities. For all patients, informed consent was obtained in accordance with protocols established by the institutional review boards (IRBs) of the University Hospitals of Cleveland or the Cleveland Clinic Foundation.

In addition, a seventh testicular sample was received from the Pathology Department at the University Hospitals of Cleveland; this sample was obtained in accordance with IRB protocols for discarded tissue samples. Patient information was unavailable in this case, but histological examination indicated normal spermatogenic progression within the tubules.

Sample Processing

Testicular samples were processed following modifications of the technique of Barlow and Hultén (1996), as described elsewhere (Judis et al. 2004). In brief, seminiferous tubules were gently teased apart, and the tissue was transferred to freshly prepared buffer solution (containing 30 mM Tris, pH 8.2; 50 mM sucrose; 17 mM citric acid; 5 mM EDTA; 0.5 mM dithiothreitol; and 0.1 mM phenylmethylsulphonyl fluoride, pH 8.2–8.4) and was incubated at room temperature for 45–60 min. Approximately 3–5 mm of the tissue was transferred into 20 μ l of 100 mM sucrose for further teasing, and 10 μ l of the resultant germ-cell slurry was deposited onto microscope slides coated with a 1% paraformaldehyde solution (pH 9.2; 0.14%–0.20% Triton X [Sigma]) and was incubated overnight in a humid chamber. Slides were air-dried and placed in a 0.04% PhotoFlo solution (Eastman Kodak) for 2 min and then were drained, allowed to air-dry, and immediately processed for immunostaining.

Immunostaining and FISH

Microscope slides were hydrated in 1 \times antibody dilution buffer (ADB) (containing 1% normal donkey serum [Jackson ImmunoResearch], 0.3% BSA, and 0.005% Triton X in PBS) for 30 min at room temperature. A total of 60 μ l of the primary antibody cocktail—consisting of SCP3 (1:75), CREST (MIM 181750) antisera (1:1,000), and either SCP1 (MIM 602162) (1:1,000), γ -H2AX (1:100) (UpState), SPO11 (MIM 605114) (1:75) (NeoMarkers), or RAD51 (MIM 179617) (1:75) (Santa Cruz Biotechnology) in 1 \times ADB—was overlaid on slides, and the slides were coverslipped and incubated overnight at 37°C in a humid chamber. After the primary antibody incubation, slides were washed in 1 \times ADB for 20 min at room temperature, followed by a second wash in 1 \times ADB at 4°C overnight. Slides were then overlaid with 60 μ l of the secondary antibody cocktail (fluorescein donkey anti-rabbit, rhodamine donkey anti-goat, and AMCA donkey anti-human [1:100] [Jackson ImmunoResearch] in 1 \times ADB) for 60 min at 37°C in a humid chamber. Slides were washed three times in PBS for 10 min and then were drained, mounted in Antifade (BioRad Laboratories), and coverslipped.

Leptotene and zygotene cells were identified and analyzed using a Zeiss Axiophot epifluorescence microscope (Carl Zeiss). Images were captured using the Applied Imaging Quips Pathvision System, and cell coordinates were noted for subsequent FISH analyses.

For chromosome-specific FISH studies, previously immunostained slides were refixed in 2% formaldehyde solution (Fisher Scientific) for ~12 min and were washed in PBS for 30 min at room temperature and in 2 \times SSC for 30 min. Slides were overlaid with 40 μ l of a probe cocktail consisting of directly labeled DNA paint probes

specific to particular human chromosomes (WCP8, WCP9, WCP21, and WCP22 [1:20]) in hybridization buffer (Vysis), were coverslipped, were transferred to an 85°C hot plate for 8 min, and were incubated overnight at 37°C in a humid chamber. Coverslips were soaked off in 2 \times SSC at 75°C for 2 min; slides were then transferred to 2 \times SSC at room temperature for 7 min, washed in PN buffer for 10 min, stained with 4,6-diamidino-2-phenylindole dihydrochloride (DAPI), rinsed in PN buffer, mounted in Antifade, and coverslipped. Previously imaged cells were then relocated and analyzed.

To identify telomeric repeat sequences, slides that were previously immunostained and/or analyzed by FISH were rehydrated in PBS for 5–15 min, were fixed for 2 min in 4% formaldehyde in PBS, were washed in PBS three times for 5 min, and were dehydrated in serial ethanol washes (concentrations 70%, 90%, and 100%) for 5 min each and then allowed to air-dry. A total of 60 μ l of a telomere-detecting peptide nucleic acid (PNA) probe cocktail (containing 0.069% PNA Oligomer [Applied Biosystems], 0.5% blocking agent, and 0.1% Tris) in 70% formamide was added, coverslipped, and denatured on an 80°C heating block for 3 min. Slides were incubated in the dark at room temperature for at least 4 h, washed twice in buffer (containing 70% formamide, 10 mM Tris, and 0.1% BSA) for 15 min, washed three times in Tris-buffered saline with Tween 20 (TBST) buffer for 5 min, and dehydrated in serial ethanol washes. Slides were allowed to air-dry and then were stained with DAPI, rinsed in PBS, mounted in Antifade, and coverslipped. Previously identified cells were then relocated and analyzed.

Cytological Analysis of Synapsis

We analyzed leptotene and zygotene cells for initiation and progression of synapsis, using antibodies against SCP3 (which detect a component of the axial/lateral element of the SC) and/or SCP1 (which detect a component of the transverse filament of the SC) to monitor formation of the SC. By this approach, the first three substages of prophase (leptotene, zygotene, and pachytene) are easily distinguished. Leptotene is characterized by the appearance of short, SCP3-positive, linear segments (axial elements) that coalesce as leptotene progresses; during zygotene, axial elements of homologous chromosomes continue to elongate and begin to synapse, with the points of synapsis identified by the appearance of SCP1 signals or the merger of SCP3 signals; by pachytene, synapsis is complete, with SCP1 and SCP3 colocalizing along the entire length of each of the 22 autosomes and across the pseudoautosomal region of the XY bivalent.

Operationally, we defined synapsis as the merger of homologous axial elements (detected by the merger of SCP3 signals) or the appearance of the transverse fila-

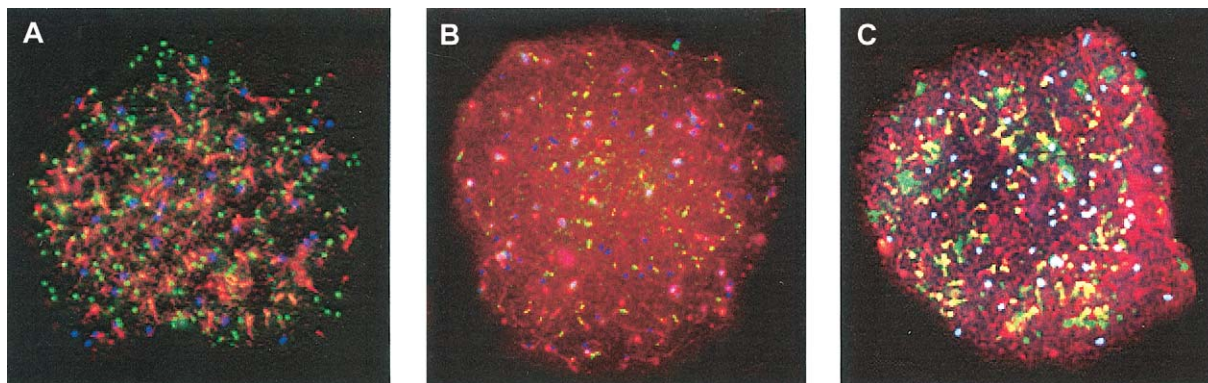


Figure 1 Immunofluorescence images of human leptotene-stage spermatocytes. SCP3 (which detects axial elements) is in red, and CREST (which detects kinetochores) is in blue. Three different markers of DSBs are shown in green: SPO11 (A), RAD51 (B), and γ H2AX (C). All three are present in leptotene nuclei, despite the fact that the axial elements are not yet fully formed.

ment (detected by SCP1). For cells in leptotene or early zygotene, we scored synaptic initiation sites, defined as punctate regions in which we observed SCP1 signals or merged SCP3 signals. In mid- and late-zygotene-stage cells, we monitored progression of synapsis, visualized by the elongation of SCP1 signals and/or the elongation of merged SCP3 signals.

Results and Discussion

We analyzed synapsis in seven individuals, scoring 8–71 leptotene- or zygotene-stage cells per individual (table 1). Since we were interested in the progression of synapsis, we chose cells in which bivalents were asynapsed or partially synapsed. At leptotene, we typically were able to score 3–4 bivalents per cell; at zygotene, we arbitrarily restricted our analyses to cells in which at least five nonacrocentric chromosomes and/or at least two acrocentric chromosomes were incompletely synapsed. In total, we analyzed 109 bivalents from 30 leptotene-stage cells and 4,800 bivalents from 286 zygotene-stage cells. As discussed below, the general features of synapsis were similar among all individuals; therefore, except as indicated, analyses were based on pooled observations from all seven individuals.

The Initial Events of Meiotic Recombination Precede Synapsis in Males

In our initial studies, we were interested in determining the temporal relationship between the recombination and synaptic pathways—in particular, determining which comes first, synapsis or recombination. Until recently, it has been assumed that the initial events of meiosis involve pairing and synapsis of homologs, with the SC providing the template for subsequent recombinational processes (e.g., the formation of double-strand breaks

[DSBs], strand invasion, and repair of DSBs). This view is supported by molecular studies of meiosis in *D. melanogaster* and *Caenorhabditis elegans*, which indicate that the initial event in meiotic recombination—DSB formation—occurs after the formation of the mature, tripartite SC and that the SC can form in the absence of DSBs (Dernburg et al. 1998; McKim et al. 1998; McKim and Hayashi-Hagihara 1998). By contrast, in *Saccharomyces cerevisiae*, DSBs occur before the formation of the SC and, indeed, are required for normal development of the SC (Sym and Roeder 1994; Roeder 1997). Similarly, recent studies of the mouse (Mahadevaiah et al. 2001) and the human female (Lenzi et al. 2005) indicate that DSBs precede SC formation, which suggests that mammals follow the yeast temporal paradigm.

Thus, we were interested in determining whether DSBs form in advance of the complete SC in the human male as well. Accordingly, we monitored localization patterns of proteins known to be involved in DSB formation (SPO11, a protein responsible for catalyzing the initial DSB reaction [Keeney et al. 1997]) or in DSB processing (RAD51, a strand invasion protein [McIlwraith et al. 2000], and γ -H2AX, a histone H2A variant that becomes phosphorylated immediately after DSB formation [Rogakou et al. 1998; Mahadevaiah et al. 2001]) with the patterns of proteins associated with the formation of the SC (SCP1, a component of the transverse filament [Liu et al. 1996], and SCP3, a component of the axial elements [Lammers et al. 1995]). As shown in figure 1, all three markers of DSBs (SPO11, RAD51, and γ -H2AX) were present in early-leptotene cells, indicating that the recombinational pathway had already been activated. In contrast, SCP1 was not detected in any early-leptotene preparations (data not shown), and SCP3 was observable only as diffuse patterns of localization, with individual SCP3 signals being present as punctate foci

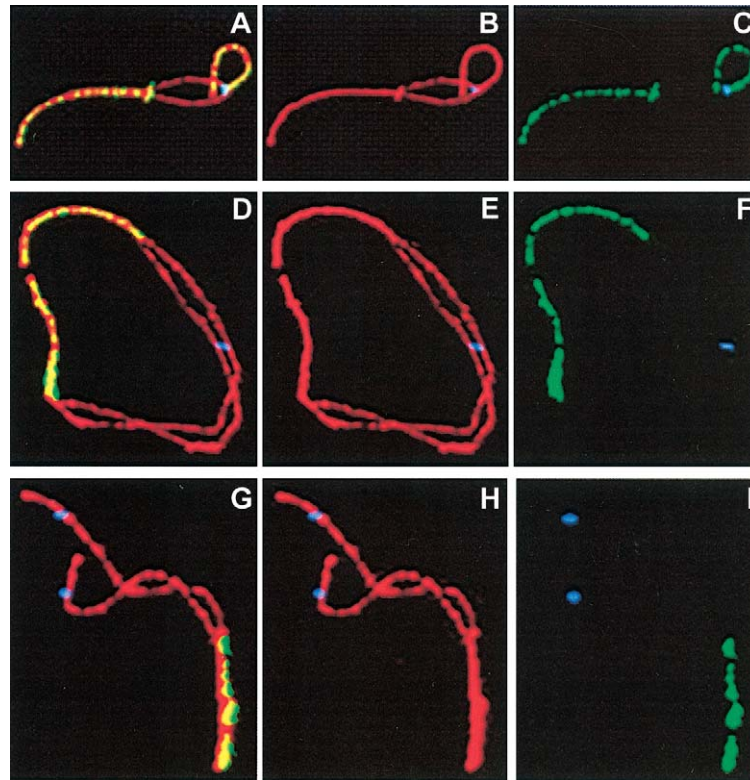


Figure 2 Localization patterns of SCP1 and SCP3 on partially synapsed submetacentric (A–C), metacentric (D–F), and acrocentric (G–I) bivalents. SCP1 (which detects the transverse filament) is in green, SCP3 (which detects axial elements) is in red, and CREST (which detects kinetochores) is in blue. In comparing the merged images (*left panels*) with images highlighting either SCP3 (*middle panels*) or SCP1 (*right panels*), it is clear that SCP1 localizes only to chromosomal sites where the two axial elements have already merged.

or short linear fragments. Thus, neither component of the SC had been built by this point, despite the fact that the recombinational process had already begun. From this, we conclude that, in human males, as in human females, mice, and budding yeast, the initial events in the recombinational pathway do not depend on the presence of the mature, tripartite SC.

Synapsis Proceeds from the Distal Regions of Human Chromosomes

In a second set of experiments, we were interested in determining whether specific chromosomal sites are important in the initiation of synapsis in human males. The telomere has long been suggested to be the site of synaptic initiation in both males and females (e.g., see Rasmussen and Holm 1978; Speed 1984; Wallace and Hultén 1985; Speed and Chandley 1990; Barlow and Hultén 1996). As part of the meiotic rearrangement of chromosomes in prophase, mammalian telomeres cluster at the nuclear envelope to form a “bouquet” during the leptotene/zygotene stage (Zickler and Kleckner 1998). Scherthan et al. (1996) showed that, in male mice, the bouquet facilitates pairing between chromosomes at the leptotene-

zygotene transition. This suggests that synapsis might also be initiated at the telomeric regions shortly after homologs begin to pair.

We tested this hypothesis by examining the number and location of synaptic initiation sites, defined operationally as short regions of merged SCP3 signals (i.e., merged axial elements) or the appearance of SCP1 signals (i.e., the appearance of the transverse element). For most individuals, the results were based solely on the SCP3 data. However, to be certain that these data were consistent with those obtained using SCP1, one individual (Sp1006) was analyzed using both SCP3 and SCP1. The data were compared, and the results were virtually identical (fig. 2), indicating that the two approaches are equivalent.

Using this approach, we first examined the distribution of synaptic initiation sites on nonacrocentric autosomes (i.e., chromosomes 1–12 and 16–20). We analyzed 286 zygotene-stage cells from the seven individuals, yielding a total of 3,734 analyzable bivalents involving nonacrocentric chromosomes. Of these, 2,191 consisted of a single uninterrupted linear SC; these were scored as completely synapsed and were not considered

further. We then focused on the remaining 1,543 bivalents, for which the axial elements were separated from one another along at least a portion of the SC (see table 2 and fig. 3A). These bivalents fell into one of four categories, and the vast majority were synapsed at both ends of the chromosomes but contained a single, asynaptic “bubble” located interstitially (table 2). Specifically, (1) in nearly 30% (440/1,543) of cases, SC formation was complete for part of the short and long arms, but there was a bubble encompassing both the p- and q-arm pericentromeric regions (fig. 3B); (2) in >40% (682/1,543) of cases, SC formation was complete for the p arm, but a bubble extended from the centromere onto the q arm (fig. 3C); (3) in ~10% (182/1,543) of cases, the bubble was restricted to the interstitial region of the q arm, with the p arm and the proximal q arm being completely synapsed (fig. 3D); and (4) in ~15% (239/1,543) of cases, more-complicated synaptic patterns were observed. These included bivalents that were paired but not synapsed (fig. 3E), bivalents with asynapsed ends (fig. 3F), and bivalents with two or more bubbles (fig. 3G).

These results indicate that, at least for the human male, there are typically two synaptic initiation sites on nonacrocentric chromosomes. One is located distally on the p arm and one distally on the q arm, and the SC then “zippers up” proximally from these sites. This process appears to be constant for all chromosomes, since we saw no obvious effect of chromosome shape (metacentric or submetacentric) or size on the number or location of initiation sites.

In contrast, acrocentric autosomes (i.e., chromosomes 13–15, 21, and 22) initiated synapsis only at the distal region of the q arm. We analyzed 1,066 acrocentric bivalents from the seven individuals; >65% (729/1,066) of these bivalents were completely synapsed. Of the remaining 337 partially synapsed bivalents, one structure was repeatedly detected: asynaptic “forks” in which merged SCP3 signals were observed for varying segments of the long arm, with the proximal regions of the q arm and the p arm being asynapsed (table 3 and fig. 4A). This pattern was observed in >85% (287/337) of the partially synapsed bivalents. In the remaining 50 in-

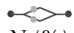
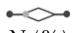
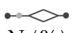
stances, more-complex synaptic patterns were observed, including interstitial initiation sites in addition to the distal site and unsynapsed bivalents (fig. 4B).

These analyses indicate that, for both nonacrocentric and acrocentric chromosomes, terminal regions play a crucial role in synaptic initiation in male meiosis. However, there is an important caveat to this interpretation. Specifically, the majority of our observations came from mid- or late-zygotene-stage cells; consequently, they were biased toward bivalents in which the synaptic process was nearing completion. Thus, it is possible that we failed to identify interstitial synaptic initiation sites because they had already zippered up. However, in subsequent studies of leptotene-stage cells (described below), telomeric initiation sites again predominated, suggesting that interstitial regions are, indeed, relatively unimportant to human male synapsis.

Our results also make it clear that there are chromosome-specific differences in synapsis: nonacrocentric chromosomes invariably have two initiation sites, one per chromosome arm, whereas acrocentric chromosomes have only one initiation site, located on the q arm. Indeed, synapsis of the p arm without complete synapsis of the q arm and centromere was never observed for an acrocentric bivalent, which suggests that acrocentric p arms are incapable of seeding synapsis. This is consistent with previous electron microscopic studies of human fetal oocytes, in which synapsis was observed to begin at q-arm termini and to proceed through the centromere to the p arms (Wallace and Hultén 1985). Possibly, this helps to prevent synapsis between nonhomologous acrocentrics, thus reducing the likelihood of de novo Robertsonian translocations.

In general, our observations agree with results previously obtained in electron microscopic analyses (e.g., see Rasmussen and Holm 1978) and immunofluorescence analyses (e.g., see Barlow and Hultén 1996) of human spermatocytes, both of which pinpointed telomeric regions as the sites of synaptic initiation. In addition, Rasmussen and Holm (1978) noted a delay in the pairing of the short arms of acrocentric chromosomes, which is consistent with our observations, and Barlow and Hul-

Table 2
Synapsis of Nonacrocentric Chromosomes

Sample	No. of Partially Synapsed Bivalents, N	 N (%)	 N (%)	 N (%)	Other N (%)
Sp370	44	10 (22.7)	24 (54.5)	3 (6.8)	7 (15.9)
Sp389	28	2 (7.1)	16 (57.1)	3 (10.7)	7 (25.0)
Sp393	107	17 (15.9)	47 (43.9)	13 (12.1)	30 (28.0)
Sp401	385	107 (27.8)	183 (47.5)	39 (10.1)	56 (14.5)
Sp403	231	73 (31.6)	101 (43.7)	26 (11.3)	31 (13.4)
Sp407	348	69 (19.8)	157 (45.1)	39 (11.2)	83 (23.8)
Sp1006	400	162 (40.5)	154 (38.5)	59 (14.7)	25 (6.2)
Total	1,543	440 (28.5)	682 (44.2)	182 (11.8)	239 (15.5)

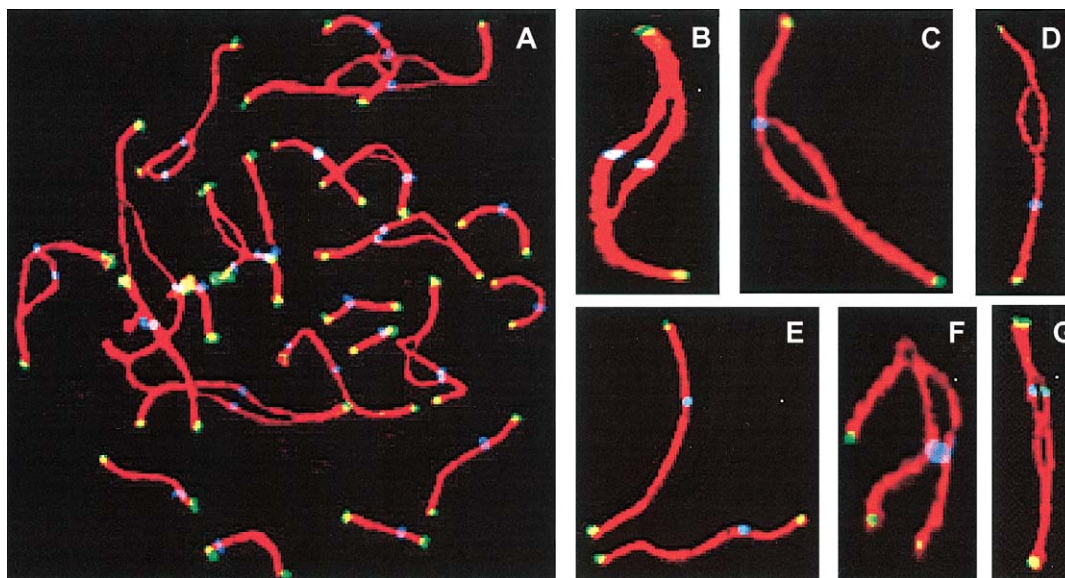


Figure 3 Synapsis of nonacrocentric chromosomes. SCP3 (which detects axial elements) is in red, CREST (which detects kinetochores) is in blue, and sequences detected by a pantelomeric PNA probe are in yellow. *A*, Representative zygotene-stage cell with both synapsed and partially synapsed bivalents. *B–G*, Various synaptic configurations observed in individual zygotene bivalents. The three common bubble structures (see table 2) are shown (*B–D*), as are a partially paired but not synapsed bivalent (*E*) and more-complicated synaptic configurations (*F* and *G*).

tén (1996) observed “ballooning axial elements” similar to our bubble structures. Thus, the basic conclusions of all three analyses are similar. However, the previous analyses were limited in at least two respects: first, by sample size, because the study of Rasmussen and Holm (1978) was based on three-dimensional reconstructions of only 39 cells and the study of Barlow and Hultén (1996) was based on a single individual, and, second, by study design, since neither analysis was intended to examine genomewide patterns of synapsis. Thus, the present report is the first to demonstrate a set number of synaptic initiation sites on individual chromosomes and the first to detail the differences between nonacrocentric and acrocentric chromosomes.

Synapsis Initiated Subtelomerically, Not at the Telomere Proper

Although our initial analyses implicated the telomere in synaptic initiation, it was unclear whether the telomere proper or the subtelomeric region was the important determinant. Thus, a subsequent set of experiments was performed to distinguish between these two possibilities.

We used pantelomeric PNA probes to localize the telomeric repeat sequences (TTAGGG) of previously immunostained leptotene-stage cells. At this stage, the axial elements are still incompletely formed, consisting of multiple short linear fragments; therefore, this represents the earliest stage at which synaptic initiation can be easily

visualized (fig. 5A). We analyzed 109 informative bivalents from 30 leptotene cells and, in the vast majority of cases, found that synaptic initiation sites were located proximal to the telomeric signals (PNA foci) (fig. 5B–5D). Specifically, in 44.9% (49/109) of cases, we observed short regions of asynapsed axial elements between the merged SCP3 signals and two distinct telomeric signals (fig. 5B and 5C), whereas, in an additional 46.8% (51/109) of bivalents, doublet telomeric signals were located immediately adjacent to merged SCP3 signals (fig. 5D). In only 8.2% (9/109) of cases were initiation sites telomeric, without adjacent merged SCP3 signals (fig. 5E and 5F).

These results indicate that synapsis proceeds from sites located in subtelomeric regions and not at the telomeres proper. However, the way in which this occurs is not yet known, nor is it clear why there is variation in the distance between the telomere proper and the synaptic initiation sites. Possibly, there are chromosome-specific determinants, with each chromosome having specific sequences that “seed” synaptic initiation. If the location of these sequences varies among chromosomes, this could explain the variation in telomere initiation-site distances that we observed. Alternatively, it may be that there is no sequence specificity to synaptic initiation; instead, there may simply be a preference for the subtelomeric region, possibly attributable to chromatin modifications that make the region more accessible. Our study was not designed to distinguish between these possibilities,

since we made no attempt to examine the location of synaptic initiation sites on specific chromosomes (i.e., by using FISH). However, this is clearly a straightforward exercise and will be an important first step in the characterization of the genomic determinants that direct synapsis in humans.

The Centromere Impedes Synapsis across Chromosome Arms

Our analysis of nonacrocentric chromosomes indicated that synapsis begins distally and proceeds toward the center of the chromosome. Assuming that synaptic initiation occurs relatively synchronously for long and short arms and that synapsis proceeds at a constant rate, we would expect to see two types of bubbles, depending on the shape of the chromosome: for metacentric chromosomes, the centromeric region would be the last to synapse, whereas, for submetacentric chromosomes, the middle of the chromosome (and hence the bubble) would be positioned somewhere on the long arm.

As described above, we did indeed identify both types of bubbles (table 2 and fig. 3). Approximately one-third of all bubbles included the centromere (fig. 3A), as expected because, of the 17 nonacrocentric chromosomes, 5 (chromosomes 1, 3, 16, 19, and 20) are metacentric or nearly so. Surprisingly, however, only 12% of nonacrocentric bivalents exhibited a bubble on the long arm (fig. 3C). Instead, we observed a third, more common type of bubble, in which the p arm was completely synapsed but in which there was a bubble that extended distally from the q-arm pericentromeric region (fig. 3B). That is, in these instances, it appeared that synapsis had proceeded from the distal p arm to the centromere but that the centromere had acted as a stop sign, prohibiting further progression onto the proximal q arm.

As this third type of bubble appeared to be restricted to submetacentric chromosomes, we decided to investigate it further by focusing on two specific C-group chromosomes, one with a large block of pericentromeric heterochromatin (chromosome 9) and one without (chromosome 8). We used FISH to identify 43 partially syn-

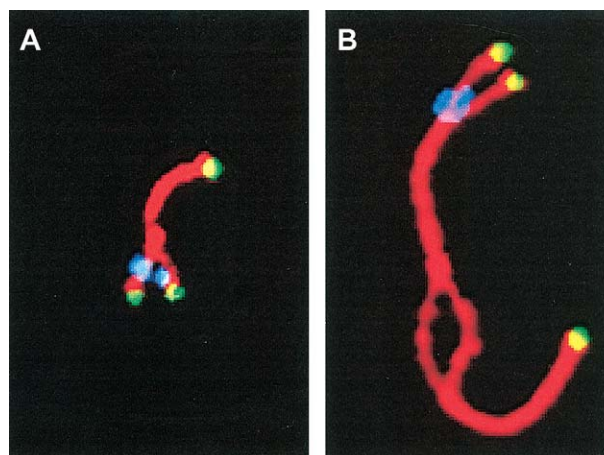

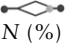


Figure 4 Synapsis of acrocentric chromosomes. SCP3 (which detects axial elements) is in red, CREST (which detects kinetochores) is in blue, and sequences detected by a pantelomeric PNA probe are in yellow. In almost all partially synapsed acrocentric chromosomes, synapsis proceeded from the q-arm terminus toward the centromere (A), although, rarely, interstitial asynaptic regions were observed (B).

apsed chromosome 9 bivalents from two individuals (Sp401 and Sp407) and 36 chromosome 8 bivalents from two individuals (Sp403 and Sp1006) and examined the location of asynaptic bubbles. For each chromosome, the results were similar to our previous observations. For chromosome 9, in almost all instances (39/43), we observed fully synapsed p arms, with asynaptic regions of variable lengths extending from the pericentromeric region of 9q. In each of the remaining four cases, we observed a relatively large bubble encompassing both proximal 9p and much of 9q; although this could represent a different pattern of synapsis, it may also be that the bivalents were simply at an earlier stage of synapsis and would have later adopted the bubble configuration observed for the other 39 bivalents. Similarly, 23 of 36 chromosome 8 bivalents demonstrated complete synapsis of the p arm, with the asynaptic bubble extending distally from the centromeric region of the q arm, and,

Table 3

Synapsis of Acrocentric Chromosomes

Sample	No. of Partially Synapsed Bivalents, N	 N (%)	 N (%)	Other N (%)
Sp370	32	21 (65.6)	0 (0)	11 (34.4)
Sp389	2	2 (100)	0 (0)	0 (0)
Sp393	26	23 (88.5)	0 (0)	3 (11.5)
Sp401	66	55 (83.3)	0 (0)	11 (16.7)
Sp403	41	33 (80.5)	0 (0)	8 (19.5)
Sp407	95	87 (91.6)	0 (0)	8 (8.4)
Sp1006	75	66 (88.0)	0 (0)	9 (12.0)
Total	337	287 (85.2)	0 (0)	50 (14.8)

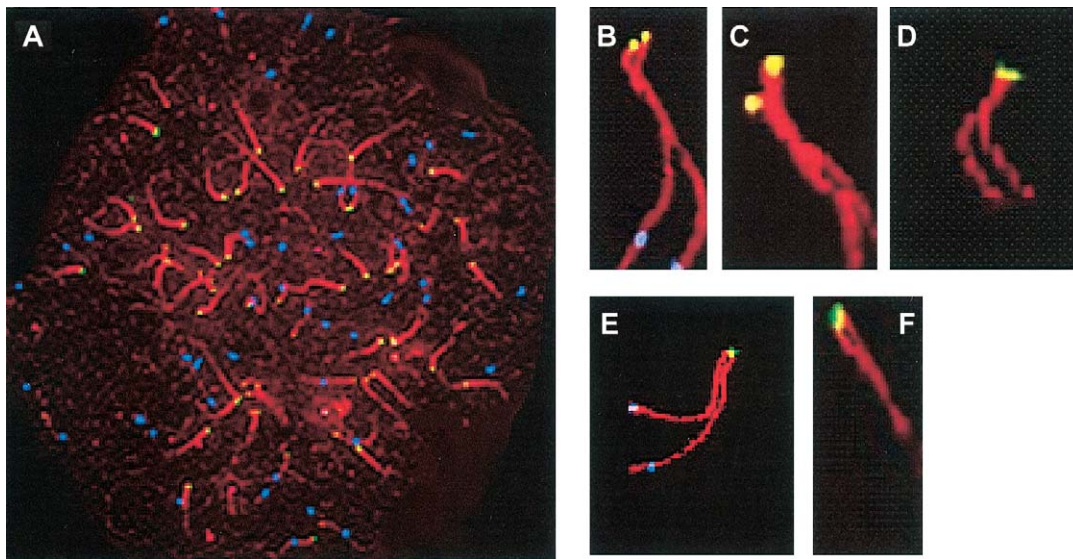


Figure 5 Analysis of sites of synaptic initiation in leptotene-stage spermatocytes. SCP3 (which detects axial elements) is in red, CREST (which detects kinetochores) is in blue, and sequences detected by a pantelomic PNA probe are in yellow. *A*, Representative leptotene-stage cell showing early stages of synapsis. In most informative bivalents, merged SCP3 signals were observed some distance from two distinct telomeric signals (*B–C*) or the telomere appeared as a doublet (*D*); rarely, synapsis appeared to begin at the telomere (*E* and *F*).

in 6 other cases, the bubble encompassed both the p and q arms, possibly indicating a bivalent at an early stage of synapsis. Only 7 of the 36 bivalents showed the morphology expected for partially synapsed submetacentric chromosomes—that is, a bubble located in the middle of 8q.

Taken together, our observations of nonacrocentric chromosomes in general, and of chromosomes 8 and 9 in particular, suggest that the centromere acts as a barrier to synapsis. Because our evidence for this effect is limited to observations of submetacentric chromosomes, it is formally possible that this phenotype is restricted to certain chromosomes. However, we think this is unlikely. Instead, we propose that all centromeres share this property but that it is simply more difficult to document on some chromosomes. That is, the p arms of acrocentric chromosomes are apparently unable to seed synapsis, making it impossible to visualize movement from the p telomere toward the centromere, and, on metacentric chromosomes, we anticipate that synapsis occurs relatively synchronously for both p- and q-arm pericentromeric regions, meaning that the centromeric region is the last to synapse.

If our conclusions are correct, they indicate a basic difference between synapsis and crossing-over in the way in which signals are propagated. That is, they indicate that the centromere interferes with the spread of synapsis, at least across part of the chromosome. In contrast, there is little evidence that crossover interference

operates across the centromere in humans. For example, in a genome-wide genetic linkage analysis, Broman and Weber (2000) were unable to find any impact of the centromere on recombination levels and, in our immunofluorescence analyses of pachytene-stage spermatocytes, we observed no effect of the centromere on the location and distribution of MLH1 foci, a marker of crossovers (Lynn et al. 2002; A. Lynn and T. J. Hassold, unpublished observations). Thus, it appears that, at least in the pericentromeric region, there are separate determinants for synaptic progression and transmission of recombination-pathway signals.

Synapsis Occurs Similarly in Different Individuals

Tables 2 and 3 provide information on the synaptic configurations observed in each of seven individuals in our series. We observed highly significant among-individual variation in the frequency of the different types of configurations for both nonacrocentric ($\chi^2 = 103.4$; $P < .001$) and acrocentric ($\chi^2 = 14.7$; $P < .05$) chromosomes. For nonacrocentric chromosomes, the effect was largely attributable to variation in the frequency of the “other” category and to the high proportion of the first type of bubble in one individual (Sp1006). For the acrocentric chromosomes, the χ^2 value was almost entirely due to the high proportion of “other” configurations in Sp370. Since the “other” category included bivalents that were difficult to analyze or unanalyzable, as well

as those that were atypical, we think that much of the individual variation was artifactual in nature. Indeed, as there was relatively little among-individual variation in the distribution of the typical configurations, we suggest that synapsis occurs relatively uniformly among males.

This conclusion is supported by our observations on other aspects of synapsis. That is, we saw no evidence of temporal differences in synaptic progression among individuals; in all individuals, synapsis was initiated subtelomerically, with two initiation sites for nonacrocentric chromosomes and one for acrocentric chromosomes, and, in each individual, the centromere acted as an impediment to synaptic progression. Thus, although we observed individual variation in the frequency of synaptic configurations, the general features of synapsis were remarkably preserved among individuals.

Conclusions

Our examination of early-prophase spermatocytes from seven males demonstrates the importance of the subtelomeric region to synapsis. This is not particularly unexpected, since previous analyses of many organisms, including humans (e.g., see Rasmussen and Holm 1978; Speed 1984; Wallace and Hultén 1985; Barlow and Hultén 1996; Scherthan et al. 1996), have implicated the telomere in this process. However, our results indicate that sites of synaptic initiation are in subtelomeric regions, not at the telomeres themselves. Further, our results suggest that this process may be linked to recombination-associated events. That is, the number and location of synaptic initiation sites appears to be tightly regulated and, at least superficially, mimics the distribution of crossovers in the human male. Similar to crossovers (e.g., see Broman and Weber 2000; Lynn et al. 2002), there appears to be a single obligatory synaptic initiation site for p and q arms of nonacrocentric chromosomes and for q arms of acrocentric chromosomes; the p arms of acrocentric chromosomes rarely, if ever, exhibit synaptic initiation sites, and synaptic initiation sites are preferentially distally located.

However, our results also make it clear that the synaptic and recombinational pathways are regulated differently. Recombination-associated proteins are visualized in leptotene spermatocytes prior to the initiation of synapsis, and the number of DSBs (as judged by the number of SPO11 foci; see fig. 1A) far exceeds the number of synaptic initiation sites. Further, the number of synaptic initiation sites seems to be under tighter control than is the number of crossovers. Recent linkage and cytological studies of meiotic exchanges indicate substantial variation within and among individuals, with a range of ~45–60 exchanges/cell in normal males (Lynn et al. 2002; Tease and Hultén 2004; Sun et al. 2005).

That is, in addition to the obligatory crossovers on all chromosome arms (other than 13p, 14p, 15p, 21p, 22p, and XqYq), there are generally at least 5–15 “optional” exchanges per cell. In contrast, our results imply an extremely tight range of synaptic initiation sites per cell. We found little evidence for interstitially located sites, which suggests that, over the entire complement, most spermatocytes contain ~40 synaptic initiation sites. Further, this appears to be a feature of most, if not all, males, because we found a surprising lack of variation in the number or distribution of initiation sites in our series. Finally, our results indicate differences in the spreading of recombination and synaptic signals. Our observations indicate that the centromere acts as a barrier to the spread of synapsis from one chromosome arm to the other, whereas recent analyses of crossing-over provide little evidence that the centromere similarly affects recombinational events.

Thus, our results provide an initial characterization of the synaptic process in human males and make it clear that sites of synaptic initiation are not equivalent to sites of crossovers. However, it still may be the case that some, or even a majority, of synaptic initiation sites eventually mature into crossovers. By combining immunofluorescence and FISH to localize synaptic initiation sites and crossovers on individual chromosomes, we should be able to address this possibility.

Acknowledgments

This research was supported by research grants HD21341 and HD42720 (to T.J.H.). We are grateful to Dr. Sue Varmuza, for providing the CREST anti-sera; Dr. Terry Ashley, for providing the SCP3 antibodies; and Dr. Peter Moens, for providing the SCP1 (SYN1) antibody. We appreciatively acknowledge the helpful comments of Jodi Jackson, Sheila Cherry, and Patricia Hunt in the preparation of the manuscript.

Web Resources

The URL for data presented herein is as follows:

Online Mendelian Inheritance in Man (OMIM), <http://www.ncbi.nlm.nih.gov/Omim/> (for SCP3, CBAVD, CREST, SCP1, SPO11, and RAD51).

References

- Anderson LK, Royer SM, Page SL, McKim KS, Lai A, Lilly MA, Hawley RS (2005) Juxtaposition of C(2)M and the transverse filament protein C(3)G within the central element of *Drosophila* synaptonemal complex. *Proc Natl Acad Sci USA* 102:4482–4487
- Barlow AL, Hultén MA (1996) Combined immunocytogenetic and molecular cytogenetic analysis of meiosis I human spermatocytes. *Chromosome Res* 4:562–573

- (1998) Combined immunocytogenetic and molecular cytogenetic analysis of meiosis I oocytes from normal human females. *Zygote* 6:27–38
- Broman KW, Weber JL (2000) Characterization of human crossover interference. *Am J Hum Genet* 66:1911–1926
- Dernburg AF, McDonald K, Moulder G, Barstead R, Dresser M, Villeneuve AM (1998) Meiotic recombination in *C. elegans* initiates by a conserved mechanism and is dispensable for homologous chromosome synapsis. *Cell* 94:387–398
- Hassold T, Hunt P (2001) To err (meiotically) is human: the genesis of human aneuploidy. *Nat Rev Genet* 2:280–291
- Holm PB, Rasmussen SW (1977) Human meiosis I: the human pachytene karyotype analyzed by three dimensional reconstruction of the synaptonemal complex. *Carlsberg Res Commun* 42:283–323
- Hunt PA, Hassold TJ (2002) Sex matters in meiosis. *Science* 296:2181–2183
- Judis L, Chan ER, Schwartz S, Seftel A, Hassold T (2004) Meiosis I arrest and azoospermia in an infertile male explained by failure of formation of a component of the synaptonemal complex. *Fertil Steril* 81:205–209
- Keeney S, Giroux CN, Kleckner N (1997) Meiosis-specific DNA double-strand breaks are catalyzed by Spo11, a member of a widely conserved protein family. *Cell* 88:375–384
- Lammers JH, van Aalderen M, Peters AH, van Pelt AA, de Rooij DG, de Boer P, Offenberg HH, Dietrich AJ, Heyting C (1995) A change in the phosphorylation pattern of the 30000–33000 Mr synaptonemal complex proteins of the rat between early and mid-pachytene. *Chromosoma* 104:154–163
- Lenzi ML, Smith J, Snowden T, Kim M, Fishel R, Poulos BK, Cohen PE (2005) Extreme heterogeneity in the molecular events leading to the establishment of chiasmata during meiosis I in human oocytes. *Am J Hum Genet* 76:112–127
- Liu JG, Yuan L, Brundell E, Bjorkroth B, Daneholt B, Höög C (1996) Localization of the N-terminus of SCP1 to the central element of the synaptonemal complex and evidence for direct interactions between the N-termini of SCP1 molecules organized head-to-head. *Exp Cell Res* 226:11–19
- Lynn A, Koehler KE, Judis L, Chan ER, Cherry JP, Schwartz S, Seftel A, Hunt PA, Hassold TJ (2002) Covariation of synaptonemal complex length and mammalian meiotic exchange rates. *Science* 296:2222–2225
- Mahadevaiah SK, Turner JM, Baudat F, Rogakou EP, de Boer P, Blanco-Rodriguez J, Jasin M, Keeney S, Bonner WM, Burgoyne PS (2001) Recombinational DNA double-strand breaks in mice precede synapsis. *Nat Genet* 27:271–276
- McIlwraith MJ, Van Dyck E, Masson JY, Stasiak AZ, Stasiak A, West SC (2000) Reconstitution of the strand invasion step of double-strand break repair using human Rad51 Rad52 and RPA proteins. *J Mol Biol* 304:151–164
- McKim KS, Green-Marroquin BL, Sekelsky JJ, Chin G, Steinberg C, Khodosh R, Hawley RS (1998) Meiotic synapsis in the absence of recombination. *Science* 279:876–878
- McKim KS, Hayashi-Hagihara A (1998) *mei-W68* in *Drosophila melanogaster* encodes a Spo11 homolog: evidence that the mechanism for initiating meiotic recombination is conserved. *Genes Dev* 12:2932–2942
- Page SL, Hawley RS (2001) *c(3)G* encodes a *Drosophila* synaptonemal complex protein. *Genes Dev* 15:3130–3143
- Rasmussen SW, Holm PB (1978) Human meiosis II: chromosome pairing and recombination nodules in human spermatocytes. *Carlsberg Res Commun* 43:275–327
- Roeder GS (1997) Meiotic chromosomes: it takes two to tango. *Genes Dev* 11:2600–2621
- Rogakou EP, Pilch DR, Orr AH, Ivanova VS, Bonner WM (1998) DNA double-stranded breaks induce histone H2AX phosphorylation on serine 139. *J Biol Chem* 273:5858–5868
- Scherthan H, Weich S, Schwegler H, Heyting C, Härle M, Cremer T (1996) Centromere and telomere movements during early meiotic prophase of mouse and man are associated with the onset of chromosome pairing. *J Cell Biol* 134:1109–1125
- Schmekel K, Daneholt B (1998) Evidence for close contact between recombination nodules and the central element of the synaptonemal complex. *Chromosome Res* 6:155–159
- Speed RM (1984) Meiotic configurations in female trisomy 21 foetuses. *Hum Genet* 66:176–180
- Speed RM, Chandley AC (1990) Prophase of meiosis in human spermatocytes analysed by EM microspreading in infertile men and their controls and comparisons with human oocytes. *Hum Genet* 84:547–554
- Sun F, Trpkov K, Rademaker A, Ko E, Martin RH (2005) Variation in meiotic recombination frequencies among human males. *Hum Genet* 116:172–178
- Sym M, Roeder GS (1994) Crossover interference is abolished in the absence of a synaptonemal complex protein. *Cell* 79:283–292
- Tease C, Hultén MA (2004) Inter-sex variation in synaptonemal complex lengths largely determine the different recombination rates in male and female germ cells. *Cytogenet Genome Res* 107:208–215
- Wallace BM, Hultén MA (1983) Triple chromosome synapsis in oocytes from a human foetus with trisomy 21. *Ann Hum Genet* 47:271–276
- (1985) Meiotic chromosome pairing in the normal human female. *Ann Hum Genet* 49:215–226
- Yuan L, Liu JG, Hoja MR, Wilbertz J, Nordqvist K, Höög C (2002) Female germ cell aneuploidy and embryo death in mice lacking the meiosis-specific protein SCP3. *Science* 296:1115–1118
- Yuan L, Liu JG, Zhao J, Brundell E, Daneholt B, Höög C (2000) The murine *SCP3* gene is required for synaptonemal complex assembly, chromosome synapsis, and male fertility. *Molecular Cell* 5:73–83
- Zickler D, Kleckner N (1998) The leptotene-zygotene transition of meiosis. *Annu Rev Genet* 32:619–697
- (1999) Meiotic chromosomes: integrating structure and function. *Annu Rev Genet* 33:603–754